Supporting Information

Single Source Precursor Route to Nanometric Tin Chalcogenides

Veronika Brune[1,*], Nidal Raydan[2], Anja Sutorius[1], Fabian Hartl[1], Bhagyesh Purohit[2], Sweta Gahlot[2], Pascal Bargiela[2], Laurence Burel[2], Michael Wilhelm[1], Corinna Hegemann[1], Ufuk Atamtürk[1], Sanjay Mathur[1] and Shashank Mishra[2,*]

[1]University of Cologne, Institute of Inorganic Chemistry, Greinstraße 6, 50939 Cologne, Germany

[2]Université Lyon 1, IRCELYON, CNRS-UMR 5256, 2 Avenue A. Einstein, 69626 Villeurbanne, France

*Correspondence: veronika.brune@uni-koeln.de (V.B.); shashank.mishra@ircelyon.univ-lyon1.fr (S.M.)

Tab. S1. Selected cell parameters of **3**, **4**, and **1a**.

	complexes		
cell parameters	$[Sn\{(SC_2H_4)_2NMe\}_2]$ **3**	$[Sn\{(SC_2H_4)_2NEt\}_2]$ **4**	$[Sn\{SEtN(Me)EtS\}(Cl)CHCl_2]$ **1a**
empirical formulas	$SnS_4N_2C_{10}H_{22}$	$SnS_4N_2C_{12}H_{26}$	$SnS_2NCl_3C_6H_{12}$
formula weight	417.97 g/mol	445.28 g/mol	387.33 g/mol
crystal system	triclinic	monoclinic	orthorhombic
space group	$P\bar{1}$	P 21/n	Pca21
R (int)	0.0986	0.0988	0.2376
R indices (all data)	R1 = 0.0856 wR2 = 0.1431	R1 = 0,0770 wR2 = 0.0881	R1 = 0.1177 wR2 = 0.1527
goodness of fit on F^2	1.043	0.933	0.988
unit cell dimensions	a = 7.975(1) Å b = 9.827(1) Å c = 11.110(1) Å α = 82.131(7)° β = 84.825(7) ° γ = 66.447(7)°	a = 10.0.67(1) Å b = 16.462(1) Å c = 18.821(1) Å α = γ = 90° β = 98.650(3)°	a = 16.881(1) Å b = 11.803(1) Å c = 12.555(1) Å α = β = γ = 90°

volume	789.9(1) Å^3	1772.9(1)Å^3	2501.28 Å^3
Z	2	4	8

Tab. S2. selected bond length and angles.

	complexes		
Bond length [Å]	[Sn{$(SC_2H_4)_2NMe$}$_2$] **3**	[Sn{$(SC_2H_4)_2NEt$}$_2$] **4**	[Sn{SEtN(Me)EtS}(Cl)$CHCl_2$] **1a**
Sn1-S1	2.479(2)	2.464(1)	2.374(5)
Sn1-S2	2.446(2)	2.432(2)	2.383(5)
Sn1-S3	2.434(2)	2.225(1)	
Sn1-S4	2.467(2)	2.459(1)	
Sn1-N1	2.519(5)	2.579(4)	2.350(1)
Sn1-N2	2.526(5)	2.570(4)	
Sn1-C6			2.170(1)
Sn1-Cl3			2.430(4)
S1-C1	1.804(8)	1.807(5)	1.817(1)
S2-C2	1.814(8)		1.820(1)
S2-C3		1.806(6)	
S3-C6	1.820(8)		
S3-C7		1.784(5)	
S4-C9	1.804(7)	1.804(6)	
N1-C2	1.469(9)	1.465(6)	1.480(1)
N1-C4	1.477(9)	1.475(6)	
N1-C5	1.473(8)	1.479(6)	1.490(1)
N2-C8	1.473(8)	1.477(6)	
N2-C10	1.476(8)	1.456(6)	
N2-C7	1.477(9)		
N2-C8		1.477(6)	
C1-C2	1.515(1)	1.503(7)	1.480(2)
C3-C4	1.513(1)	1.505(7)	1.480(3)
C5-C6		1.510(7)	
C6-C7	1.492(1)		

C8-C7		1.470(8)	
C8-C9	1.519(9)		
C9-C10		1.512(8)	
C11-C12		1.510(8)	
Cl5-C6			1.790(1)
Cl4-C6			1.756(1)
angles [°]			
S1-Sn1-S2	109.84(7)	111.8(1)	121.2(2)
S3-Sn1-S4	110.54(7)	112.0(1)	
N1-Sn1-N2	116.12(5)	117.6(1)	
C6-Sn1-Cl3			121.3(5)
N1-Sn1-C6			94.1(6)

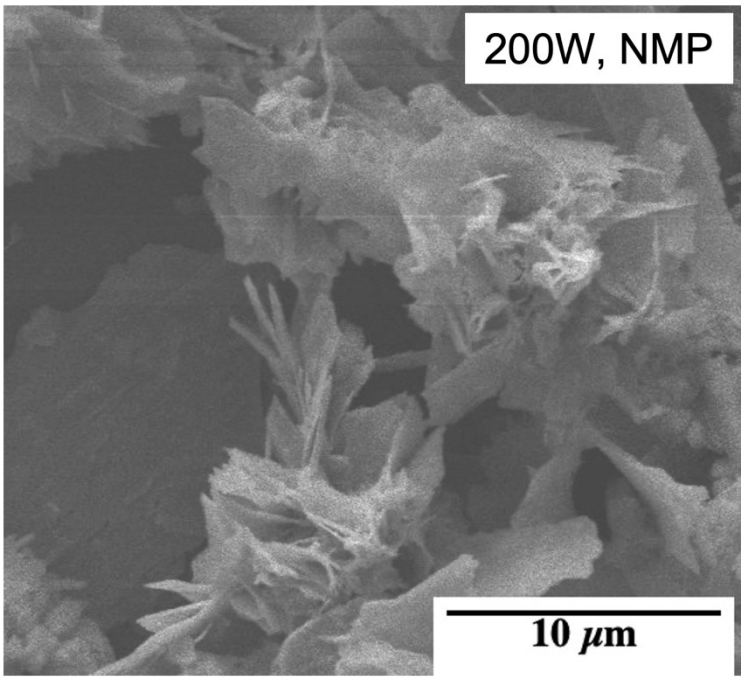

Fig. S1. SEM image of microwave deposited SnS flakes from prepared from **1**.

*XPS measurements of microwave deposited precursor [Sn{(SC$_2$H$_4$)$_2$NMe}$_2$] **3:***

The quantifications of the XPS measured microwave assisted decomposition compound **3** are in good agreement with the literature [1-4]. From the survey spectra in Fig. S2a the expected Sn (6.7 at.%) and S (20.5 at.%) peaks were observed but also remarkable amounts of carbon (62.1 at.%) and nitrogen (6.3 at.%) were detected. Additionally, a small trace of oxygen (4.4 at%) is also visible. The non-stoichiometric amount of sulfur to tin and the very high

content of carbon indicating remaining ligand fragments at the surface of the SnS_2 nanoparticles. Therefore, high-resolution spectra of sulfur (S 2p, Fig. S2b), carbon (C 1s, Fig. S1c), and tin (Sn 3d, Fig. S2d.) have been measured. The spectra of S 2p and C 1s show some remaining organic fragments, displayed by the detection of C-S and C-C, C-H bonds and the remaining amount of nitrogen observed from survey scans. These ligand fragments prevent the formed particles from agglomeration, by the repulsing effects of remaining functional groups. The high-resolution spectra of Sn and S show two different tin species, the desired SnS_2 and the mixed valence Sn_2S_3 phase. The observation of partial reduction of the tin center (Sn^{IV} to Sn^{II}) is in good agreement with before described phenomena of thermodynamically stability of the different tin phases. Consequently, 200 W seemed to be too much power for clean decomposition resulting in pure SnS_2 particles.

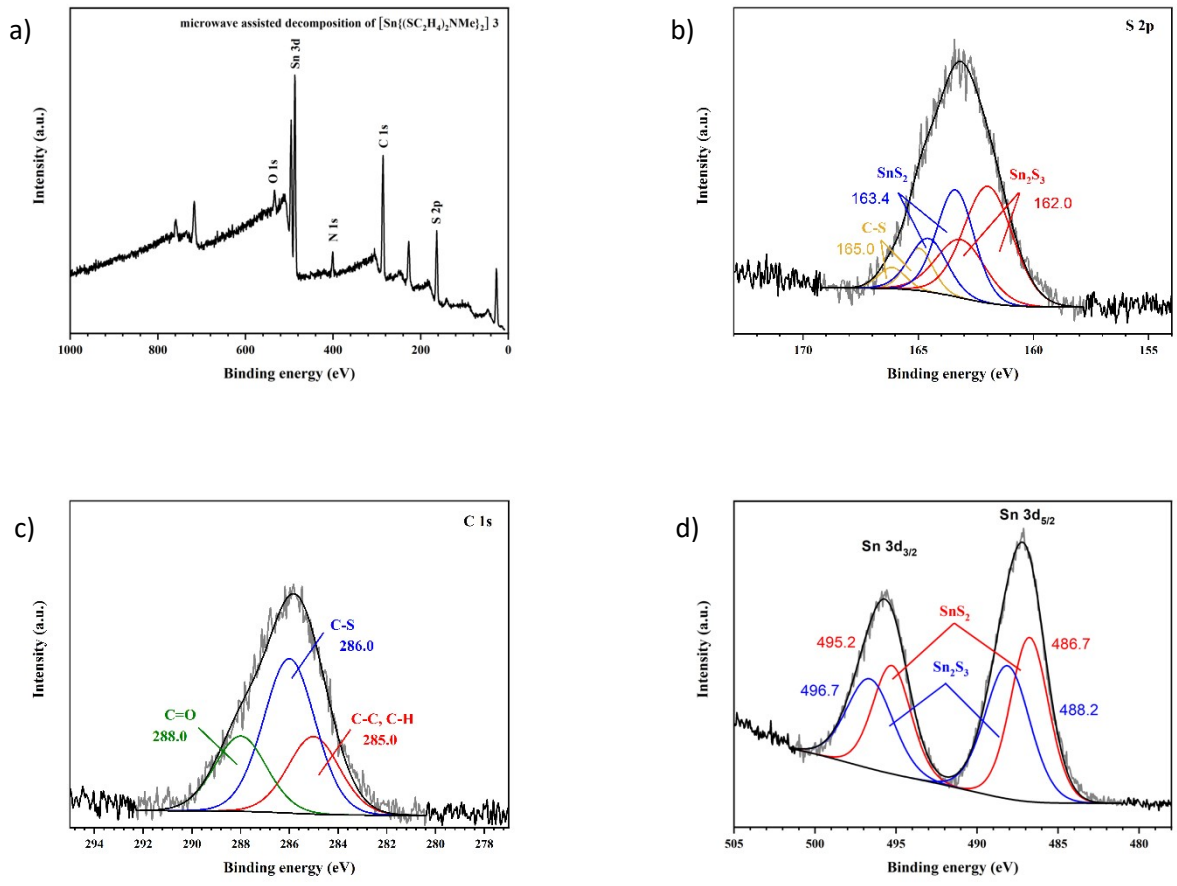

Fig. S2. XPS survey (a) and high-resolution (b-d) measurements of microwave assisted decomposition of [Sn{$(SC_2H_4)_2NMe$}$_2$] **3**.

The remining ligand fragments seem to avoid the agglomeration of formed tin particles, resulting from the repulsing effects of ligand fragments of the particle surface (Fig. S3).

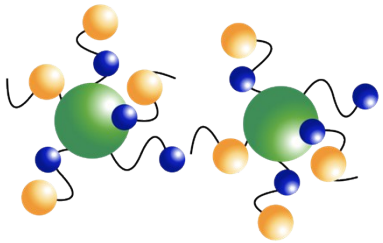

Fig. S3. Expected tin sulfide particles with ligands fragments, resulting in separated particles.

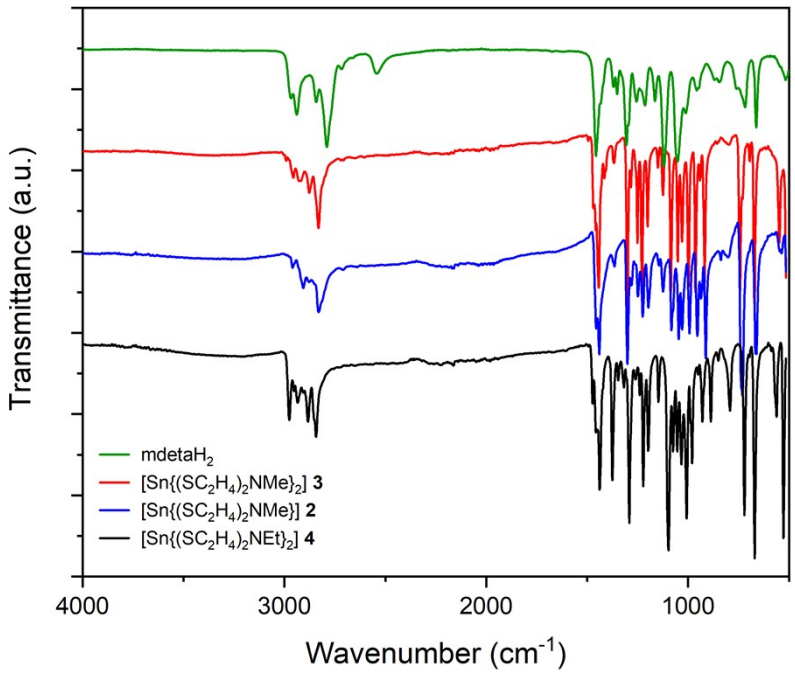

Fig. S4. FT-IR spectra of *mdetaH*$_2$ (green), **2** (blue), **3** (red) and **4** (black)**:** significant bands for *mderaH*$_2$: 2944w (C-H valence vibration), 2794s (R^1R^2N-CH_3 vibration), 2557w (S-H valence vibration), for **2**: 2911w (C-H valence vibration), 2835s (R^1R^2N-CH_3 vibration), for **3**: 2967w (C-H valence vibration), 2836w (R^1R^2N-CH_3 vibration), and for **4**: 2979-2886s (C-H valence vibration), 2846w (R^1R^2N-CH_3 and R^1R^2N-CH_2- vibration).

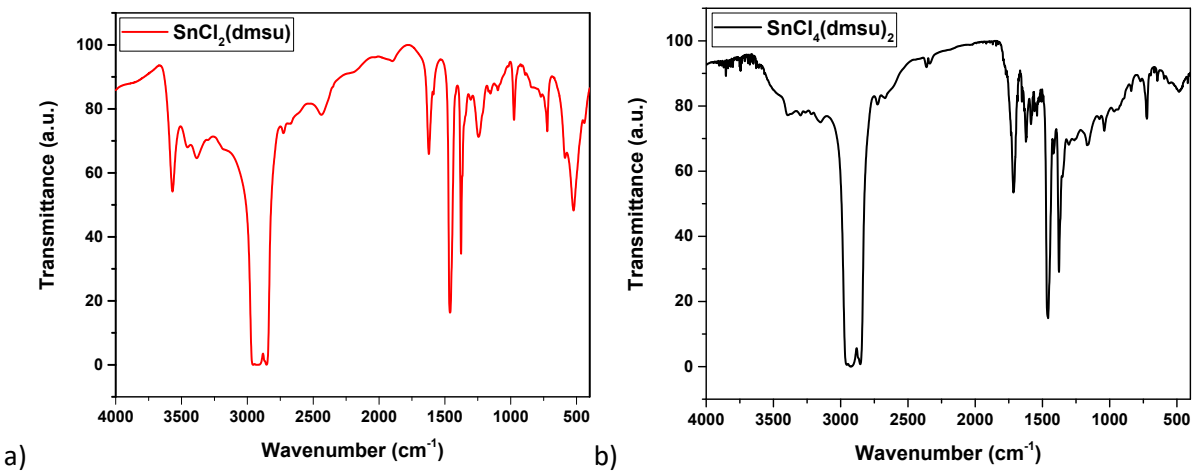

Fig. S5. FT-IR spectra of [$SnCl_2$(dmsu)] **5** (a), and [$SnCl_4(dmsu)_2$] **6** (b).

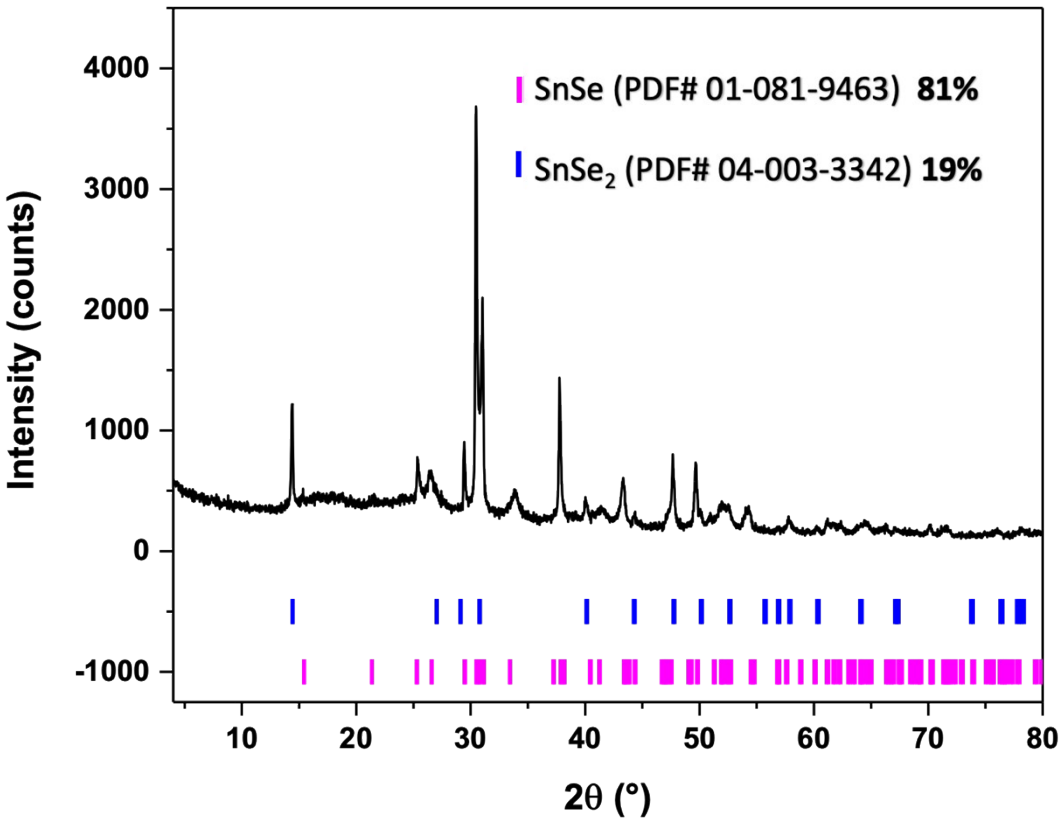

Fig. S6. Powder XRD pattern of the residue left at the end of TGA of mixed SnSe and $SnSe_2$ NPs obtained from the decomposition of **6** in oleic acid alone. It shows that the $SnSe_2$ content decreases from 61% (in the as-prepared NPs) to 19% (in the residue) due to the loss of Se during heating.

Material characterization:

X-ray photoelectron spectroscopy (XPS) measurements were performed by using an ESCA M-Probe Spectrometer from Surface Science Instruments, equipped with a monochromatic Al Kα excitation source (1484.4 eV). Survey and high-resolution spectra were referenced to the 284.8 eV for the adventitious carbon signal. After a background correction using a Shirly function, the components were fitted with a Gaussian-Lorentzian GL(30) peak shape. Qualitative and quantitative analyses were done with CasaXPS software (Casa Software Ltd.).

[1] M. Cruz, J. Morales, J. P. Espinos, J. Sanz, J. Solid State Chem. 2003, 175, 359–365.

[2] R. Godoy-Rosas, S. Barraza-Félix, R. Ramírez-Bon, R. Ochoa-Landin, H. A. Pineda-León, M. Flores-Acosta, S. G. Ruvalcaba-Manzo, M. C. Acosta-Enriquez, S. J. Castillo, Chalcogenide Lett. 2017, 14, 365–371.

[3] T. J. Whittles, L. A. Burton, J. M. Skelton, A. Walsh, T. D. Veal, V. R. Dhanak, Chem. Mater. 2016, 28, 3718–3726.

[4] M. Mirzaee, A. Dolati, J. Sol-Gel Sci. Technol. 2015, 75, 582–592.